

TOPICAL REVIEW

Precision gravimetry with atomic sensors

M de Angelis^{1,2}, A Bertoldi³, L Cacciapuotì⁴, A Giorgini^{2,5},
G Lamporesi⁶, M Prevedelli⁷, G Saccorotti⁸, F Sorrentino²
and G M Tino²

¹ Istituto di Cibernetica CNR, via Campi Flegrei 34, 80078 Pozzuoli (NA), Italy

² Dipartimento di Fisica and LENS, Università di Firenze-INFN, via Sansone 1 Polo Scientifico, I-50019 Sesto Fiorentino (Firenze), Italy

³ Laboratoire Charles Fabry de l'Institut d'Optique, CNRS, Campus Polytechnique, RD 128, F-91127 Palaiseau Cedex, France

⁴ ESA Research and Scientific Support Department, ESTEC, Keperlaan 1, PO Box 299, 2200 AG Noordwijk ZH, The Netherlands

⁵ Dipartimento di Fisica, Università di Napoli, via Cinthia, I-80126 Napoli, Italy

⁶ JILA, University of Colorado, Boulder, CO 80309-0440, USA

⁷ Dipartimento di Chimica Fisica e Inorganica, Università di Bologna, V.le Risorgimento 4, 40136 Bologna, Italy

⁸ Istituto Nazionale di Geofisica e Vulcanologia, sez. di Pisa, via della Faggiola 32, 56126 Pisa, Italy

E-mail: marella.deangelis@fi.infn.it

Received 13 February 2008, in final form 4 June 2008

Published 17 December 2008

Online at stacks.iop.org/MST/20/022001

Abstract

Atom interferometers have been shown to be very stable and accurate sensors for acceleration and rotation. In this paper we review the applications of atom interferometry to gravity measurements, with a special emphasis on the potential impact of these techniques on applied science fields.

Keywords: atom interferometry, experimental studies of gravity

(Some figures in this article are in colour only in the electronic version)

1. Introduction

Matter-wave interferometry has recently led to the development of new techniques for the measurement of inertial forces, finding important applications both in fundamental physics and applied research. The remarkable stability and accuracy that atom interferometers have reached for acceleration measurements can play a crucial role for gravimetry. Quantum sensors based on atom interferometry had a rapid development during the last decade and different schemes were demonstrated and implemented. Atom interferometry is used for precise measurements of gravity acceleration [1–3], Earth's gravity gradient [4, 5] and rotations [6, 7]. Currently, experiments based on atom interferometry are in progress on the equivalence principle test [8] and on the measurement of the gravitational constant G [9–11], while experiments on tests of general relativity [12] and of the

Newton $1/r^2$ law [13, 14] and gravitational wave detection [15–17] have been proposed.

Accelerometers based on atom interferometry have been developed for many practical applications including metrology, geodesy, geophysics, engineering prospecting and inertial navigation [5, 18, 19]. Ongoing studies show that the space environment will allow us to take full advantage of the potential sensitivity of atom interferometers [20, 21].

Among the metrological issues in gravimetry, the new definition of the unit of mass (the kilogram) depending on the Planck constant h is one of the most interesting. The link will be realized by means of a Watt balance, which will compare an electric to a mechanical power. In this scheme an accurate measurement of the acceleration of gravity is needed that can be attained by the atom interferometer sensor proposed in [22]. For the Newtonian gravitational constant G , the proposed idea is to use neutral atoms as microscopic test masses to probe the

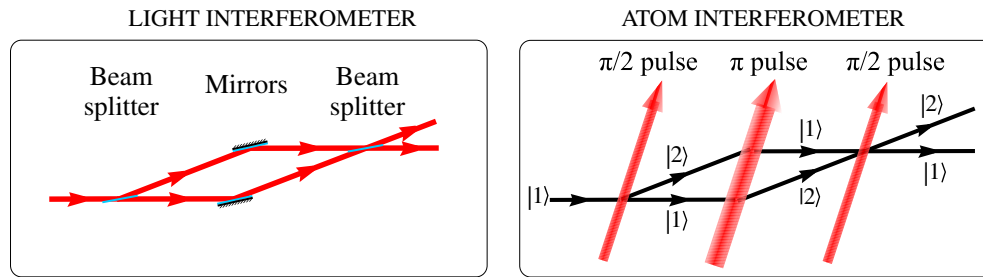


Figure 1. Analogy between an optical and an atomic Mach–Zehnder-type interferometer. Left: a light beam is split into two by a beam splitter, then two mirrors change their propagation vector to have them crossing again and a second beam splitter recombines the beams in order to observe interference between the light fields that propagated along different paths. Right: in the atomic analogue matter waves propagate and light pulses of different lengths are used as optical elements of the interferometer. The internal atomic state, $|1\rangle$ or $|2\rangle$, is coupled to the external momentum of the wave packet.

gravitational field generated by a well-characterized source mass [5, 23].

In gravity measurements, especially in geophysical applications and for reference networks, the development of absolute meters for field use is particularly important. Instruments with high long-term stability and accuracy (between 10^{-8} and 10^{-9} on a time scale between 1 year to 1 decade) would allow us to monitor long-period changes of the gravimetric signal. Gravimeters and gradiometers based on atom interferometry appear well suited for these applications because of the excellent long-term stability.

This paper discusses the applications of atom interferometry to gravity studies. In section 2, we present the general principles of operation of atom interferometers. Section 3 outlines the different applied fields in which accurate measurements of the gravity acceleration are needed. Section 4 is dedicated to the description of instruments for gravity measurements. In section 5 classical instruments for determination and mapping of the gravitational acceleration are described, most of them being commercial instruments commonly used in applied sciences. Section 6 is dedicated to the description of instruments based on light pulse atom interferometry. Future perspectives for accurate gravity measurements and global mapping of the Earth gravitational field are presented in section 7.

2. Atom sensor principle

Seminal papers on atom interferometry are [24, 25], overviews of basic principles, theoretical and experimental work can be found in [26–28] and a unified theoretical picture for gravito-inertial sensors as well as for atomic clocks can be found in [29].

It is a fundamental and well-tested feature of quantum mechanics that wave-like properties are associated with particles. Already at the time of the first Fermi's matter-wave experiment on neutrons Bragg diffraction from crystal planes [30], it was clear that neutral matter was better than charged particles or photons for realizing highly sensitive devices for inertial accelerations and/or rotations. Neutral matter is much less sensitive to perturbing electric and magnetic fields than charged particles and its typical speed can be much lower than the speed of light allowing a longer interaction time within a

fixed length scale. Neutrons however were difficult to produce in the laboratory since accelerators were needed and the dream of observing interference patterns on much more complex and massive systems like entire atoms became feasible only in the 1990s when several groups around the world demonstrated various atom interferometers [31–34].

The wavelength of the matter wave associated with an atom depends on the momentum \mathbf{p} of the atom. It is also called *de Broglie wavelength* and is given by

$$\lambda_{\text{mw}} = \frac{h}{p} = \frac{h}{Mv} \quad (1)$$

where h is the Planck constant, M is the atom mass and v its velocity. To have an idea of the dimension of such a wavelength let us consider thermal atoms with $v \simeq 10^3 \text{ m s}^{-1}$: the matter wavelength is $\lambda_{\text{mw}} \simeq (0.4/A) \times 10^{-9} \text{ m}$, where A is the mass number of the atoms. For cold atoms, at a temperature of $1 \mu\text{K}$, this wavelength becomes as large as $1 \mu\text{m}$ or more.

In analogy to optical interferometers, atomic matter waves can be split and recombined giving rise to an interference signal (see figure 1). Different schemes have been used for splitting, reflecting and recombining atomic matter waves: the atom optics components can be either material structures [31, 32] or light fields [33–35]. In the former case, the experiment is analogous to the Young's double-slit interferometer and the diffraction of the matter wave is performed by a material structure which typically requires high surface quality and precise positioning. In the latter case, the diffraction is obtained thanks to a laser standing wave generated by two counterpropagating laser beams, producing in fact a light diffraction grating. Diffraction by light fields, compared to that induced with material structures, allows for a much larger tunability thanks to the easy experimental control of parameters such as phase, intensity and lattice spacing. The diffraction light process can be generalized to several configurations. We will discuss in the next sections two of these configurations: Raman diffraction and Bloch oscillation in a standing wave, as these schemes have reported interesting results for inertial sensors.

In principle, atom interferometers can be much more sensitive to inertial forces than the corresponding sensors based on optical interferometry. This is a consequence of the considerably small group velocity of the atom compared to

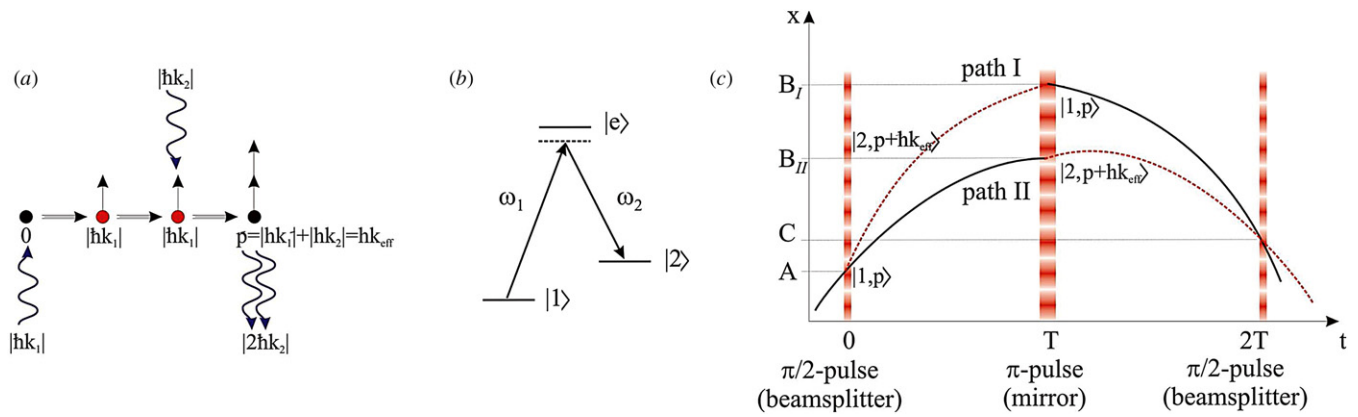


Figure 2. Atom interferometry based on Raman light pulses: (a) momentum transfer in a stimulated Raman transition; (b) simplified scheme of the atomic energy levels involved; (c) a Mach-Zehnder interferometer in spacetime plots: the atomic trajectories follow straight lines in the absence of gravity, and the parabolic curves in the presence of gravity.

the velocity of light: during the time spent by an atom inside an interferometer, an acceleration changes the length of the interfering path, thus inducing a phase shift in the interference signal. Actually, many factors limit the sensitivity of atom interferometers. In detecting the particles (atoms or photons), the sensitivity is limited by the shot noise and the minimum detectable signal scales as $1/\sqrt{N}$ where N is the number of particles. The experimental time duration for operating an atom interferometer is of the order of 1 s and the typical number of atoms contributing to the signal in each cycle is usually 10^5 – 10^7 , whereas in an optical interferometer 10 mW light power corresponds to 4×10^{16} photons s^{-1} . Moreover, beam splitters used for light can achieve a much higher quality than those for atoms. Nonetheless, atom interferometers, when measuring gravity acceleration, are nowadays competing in terms of accuracy with the best optical interferometry sensor of gravity based on freely falling corner cubes.

Laser cooling techniques have become an important experimental tool for the development of atom-interferometry-based quantum sensors. By using laser cooling techniques, atomic gases from a room temperature and low pressure vapor can be cooled to a few micro-Kelvin [36], allowing for remarkably precise control on the position and the velocity of the atomic sample. Low temperatures are important to improve both the signal-to-noise ratio of the interference signal and its sensitivity to external fields due to long interaction times. Even lower temperatures can be reached using evaporative cooling techniques. Under these conditions, the wave properties of the atoms become relevant and their behavior must be described using quantum statistics (close to the degeneration temperature) [37]. Coherent atomic sources based on ultracold atoms are presently under study to improve the performances of atom interferometry sensors [38].

2.1. Raman atom interferometry

In the first experiments that demonstrated the power of atom interferometry for accurate measurements of the Earth's gravity acceleration [1, 2] and its gradient [4], the separation and reflection of the atomic wave packet was achieved by inducing a Raman transition between internal states of the atoms by an electromagnetic field [39, 40].

Each single atom independently participates in the interferometer and the contribution of a large ensemble of atoms provides a detectable and statistically significant signal. We will briefly describe the single atom case. The state of the atom is described by a ket $|i, \mathbf{p}\rangle$, where i indicates the internal state of the atom and \mathbf{p} its external momentum. Let us consider an alkali atom as a two-level system, represented by the two hyperfine states 1 and 2 of the ground level (see figure 2). Suppose it is initially in the internal state 1 and that it is freely moving with momentum \mathbf{p} . Two counterpropagating beams, with propagation vectors \mathbf{k}_1 and $\mathbf{k}_2 \simeq -\mathbf{k}_1$, whose frequency difference is resonant with the atomic two-level system can drive a two-photon Raman transition and induce Rabi oscillations on the atom. As a function of the interaction time t the atomic state can be described as

$$|\psi(t)\rangle = \cos\left(\frac{\Omega t}{2}\right) |1, \mathbf{p}\rangle + e^{-i\frac{\pi}{2}} e^{i\phi_L} \sin\left(\frac{\Omega t}{2}\right) |2, \mathbf{p} + \hbar \mathbf{k}_{\text{eff}}\rangle \quad (2)$$

where $\hbar \mathbf{k}_{\text{eff}}$ represents the effective momentum transferred to the atom, Ω represents the effective two-photon Rabi frequency⁹ and ϕ_L is a phase term acquired during the interaction with the electromagnetic wave. The internal state of the atom and its momentum are always coupled, as a consequence of momentum and energy conservation in the system atom+photons. Two particular kinds of pulses deserve special attention:

- A $\pi/2$ -pulse, that plays the role of a matter-wave splitter, happens when $\Omega t = \pi/2$. If the atom is initially in one of the two states, the $\pi/2$ -pulse drives it into an equal superposition of the two,
- A π -pulse, that acts as a matter-wave reflector, is obtained when $\Omega t = \pi$ and it completely transfers the atom from one state to the other.

Figure 1 shows the deep analogy between a light and a matter-wave Mach-Zehnder interferometer. Consider an atom in the state $|1\rangle$ at the initial time $t = 0$; a sequence of

⁹ Typical values for these parameters are $k_{\text{eff}} = 10^7 \text{ m}^{-1}$ and $\Omega = 2\pi \times 10 \text{ kHz}$.

$\frac{\pi}{2} - \pi - \frac{\pi}{2}$ pulses first splits the atomic wave packet into two parts, they are then inverted and finally recombined in order to observe the interference signal. During the sequence the atomic wave packets independently evolve along two spatially separated trajectories under the influence of external fields, inertial accelerations and rotations.

The use of a two-photon transition with counter-propagating beams allows us to transfer a large momentum $|k_{\text{eff}}| = |k_1| + |k_2|$ to the atom increasing, in this way, the spatial separation of the two wave packets and therefore the sensitivity to accelerations.

Figure 2 shows how a sequence of three Raman pulses is used to split, redirect and recombine an atom while simultaneously changing its internal state. At the end of this sequence, the fraction of atoms in one of the states is detected. The result is an oscillatory function of the interferometer path difference, which depends on the gravitational acceleration.

The total phase difference between the two paths of the interferometer (path I and path II in figure 2) can be divided into two contributions. The first contribution, $\Delta\phi_{\text{evol}}$, describes the periods of free evolution between Raman pulses. Using Feynman path integrals formalism, valid for Lagrangians at most quadratic with respect to the position \mathbf{x} and the velocity \mathbf{v} , it can be demonstrated [41] that the evolution of the wavefunction of a quantum system in an external potential $V(\mathbf{x})$ from (\mathbf{x}_A, t_i) to (\mathbf{x}_B, t_f) is determined by the quantum propagator $\sum_{\Gamma} e^{iS_{\Gamma}/\hbar}$, where Γ represents all the possible paths and S_{Γ} is the action along the path Γ . In the classical limit the action

$$S_{\Gamma} = \int_{t_i}^{t_f} \mathcal{L}[\mathbf{x}(t), \dot{\mathbf{x}}(t)] dt \quad (3)$$

is much greater than \hbar . In this case, only the paths close to the classical ones interfere constructively and the resulting phase shift is simply given by the differential action evaluated along the two possible paths:

$$\Delta\phi_{\text{evol}} = \frac{S_{II} - S_I}{\hbar} = \frac{1}{\hbar} \oint_{\Gamma_0} \mathcal{L} dt, \quad (4)$$

where Γ_0 indicates the whole classical interferometer path.

The second contribution, $\Delta\phi_{\text{laser}}$, contains the phase terms that are imprinted in the atomic wavefunction at the four spacetime points where the atom interacts with the interferometer light pulses. Whenever the state of the atom changes during such an interaction, it acquires an additional phase $\phi(\mathbf{x}, t) = \mathbf{k}_{\text{eff}} \cdot \mathbf{x} - \omega_{\text{eff}} t$, where \mathbf{x} is the position of the atom at time t . For a complete interferometer sequence, $\mathbf{x}^A, \mathbf{x}_I^B, \mathbf{x}^C$ and $\mathbf{x}^A, \mathbf{x}_{II}^B, \mathbf{x}^C$ being the positions of the atom at the times 0, T , $2T$ along the two interferometer paths, it results

$$\Delta\phi_{\text{laser}} = \phi(\mathbf{x}^A, 0) - \phi(\mathbf{x}_I^B, T) - \phi(\mathbf{x}_{II}^B, T) + \phi(\mathbf{x}^C, 2T). \quad (5)$$

Any external force induces an acceleration on the atomic motion and, consequently, a displacement of the atom relative to the laser wavefronts. Let us consider a vertical Raman interferometer on an atom that is freely falling under the effect of the gravity acceleration g , supposed constant and uniform in the interferometer region. This approximation implies that

$\Delta\phi_{\text{evol}}$ vanishes. If the starting conditions are $z(0) = 0$ and $v(0) = v_0$ we have

$$\begin{aligned} \phi(\mathbf{x}^A, 0) &= 0 \\ \phi(\mathbf{x}_I^B, T) &= k_{\text{eff}} \left[-\frac{1}{2} g T^2 + v_0 T \right] \\ \phi(\mathbf{x}_{II}^B, T) &= k_{\text{eff}} \left[-\frac{1}{2} g T^2 + \left(v_0 + \frac{\hbar k_{\text{eff}}}{m} \right) T \right] \\ \phi(\mathbf{x}^C, 2T) &= k_{\text{eff}} \left[-2g T^2 + \left(2v_0 + \frac{\hbar k_{\text{eff}}}{m} \right) T \right] \end{aligned} \quad (6)$$

resulting in an interferometer phase shift induced by local gravity g of

$$\Delta\phi_g = -k_{\text{eff}} g T^2. \quad (7)$$

A more precise calculation taking into account the evolution of the wave packet during the finite length pulses of the interferometer has been done in [42].

In the case of non-uniform fields, an additional contribution due to the non-perfect overlap of the two wave packets at the end of the interferometer has to be considered. Interference occurs anyway though, thanks to the extended spatial coherence of the atomic wavefunction. We can express gravity considering a reference value $-g$ for the acceleration in $z = 0$ and a constant gradient γ ($\sim 3 \times 10^{-6} \text{ s}^{-2}$). Any freely falling body will then have the following equation of motion $\ddot{z}(t) = -g + \gamma z(t) + z(0)$. With this linear gradient approximation, the path integral approach can be applied considering an unperturbed system with uniform gravity and a perturbation to the Lagrangian $\Delta\mathcal{L} = -\frac{1}{2} m \gamma z^2$. The calculation leads to a further shift induced by the gravity gradient that adds up to the uniform gravity one. This perturbation phase term is expressed by

$$\Delta\phi_{\text{grad}} = k_{\text{eff}} \gamma T^2 \left(\frac{7}{12} g T^2 - v_0 T - z_0 \right). \quad (8)$$

The term introduced by the gradient is $\sim \frac{7}{12} k_{\text{eff}} \gamma g T^4$. For most of the atom interferometer experiments this term is $\sim 3 \times 10^{-8}$ times the dominant one.

An exact analytical phase shift expression for atom interferometers can be found in [43], where the authors use atom optics *ABCD* formalism. Results of this review are valid for a time-dependent external Hamiltonian at most quadratic with respect to the position \mathbf{x} and the velocity \mathbf{v} .

The sensitivity to gravity can be maximized by performing the measurement with atoms and beams propagating along the vertical axis. The interferometer is operated when the atoms are freely falling and this limits the whole duration of the interferometer sequence for a given size of the experimental apparatus. Long interrogation times T are desired in that they increase the sensitivity to accelerations in the phase measurement as shown in equation (7). The other way to enhance the interferometer performances is to transfer larger momentum k_{eff} . A way to achieve this is replacing each pulse with a sequence of pulses [44, 45].

Figure 3 shows a scheme of a cold atom gravimeter and the interference fringes obtained by scanning the phase difference of the reference Raman lasers. The Raman transition between the two states can be induced using two laser beams whose

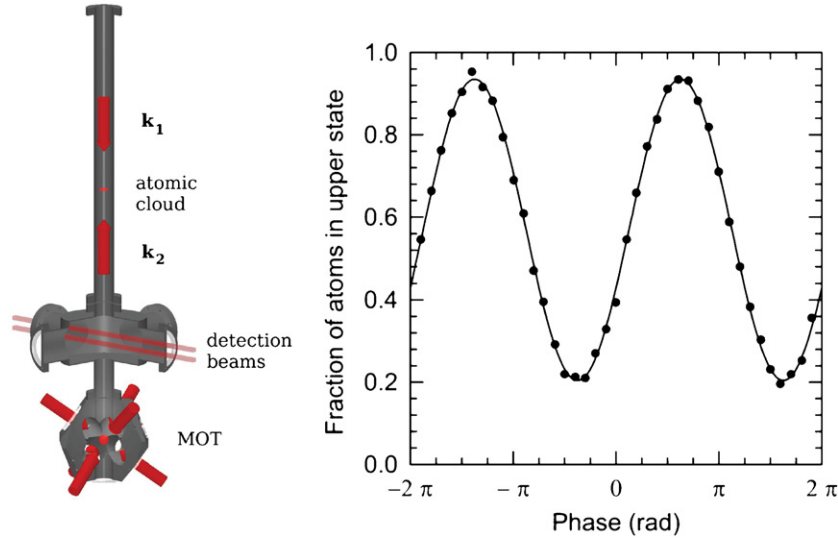


Figure 3. Experimental setup of an atom interferometer and interference fringes obtained by scanning the relative phase of the Raman lasers. The atom fringes have been recorded in the gravity experiment in Stanford [2]. Experiment interrogation time between the light pulses is $T = 160$ ms. Each of the 40 data points represents a single launch of the atoms, spaced 1.3 s apart and taken over a period of 1 min.

frequency difference is phase-locked to a stable microwave source [46]. Alternatively, optical modulators can be used to produce the required frequencies [1].

Optics vibrations along the Raman beams path can dramatically affect the acceleration measurement, as the Raman beams wavefronts represent the reference frame in which the measurement of the acceleration is performed. For this reason minimizing the ‘not common’ optical path for the two beams and stabilizing the remaining optics from seismic vibrations (in the 0.1–10 Hz range) are essential experimental requirements.

2.2. Atom Bloch oscillation

When a sample of atoms interacts with a laser standing wave generated by two counterpropagating laser beams, the standing wave acts as a diffraction grating for the atoms. In such regular structures created by interfering laser beams the atoms can be trapped by the dipole force. In particular, under the influence of a periodic potential and a weak uniform force, the atomic momentum changes periodically, a phenomenon known as Bloch oscillations. Bloch oscillations were predicted for electrons in a periodic crystal potential in the presence of a static electric field [47] but could not be observed in natural crystals because of the scattering of electrons by the lattice defects. They were directly observed using atoms in an optical lattice in [48].

Bloch oscillations are a pure quantum effect which can be explained in a simple one-dimensional model. The periodicity of the lattice (period d) leads to a band structure of the energy spectrum of the particle and the corresponding eigenenergies $E_n(q)$ and eigenstates $|n, q\rangle$ (Bloch states) are labeled by the discrete band index n and the continuous quasi-momentum q ; $E_n(q)$ and $|n, q\rangle$ are the periodic functions of q with period $2\pi/d$ and q is conventionally restricted to the first Brillouin zone $[-\pi/d, \pi/d]$. Under the influence of a constant external force F , weak enough not to induce interband transitions, a

given Bloch state $|n, q(0)\rangle$ evolves (up to a phase factor) into the state $|n, q(t)\rangle$ according to

$$q(t) = q(0) + Ft/\hbar. \quad (9)$$

This evolution is periodic with a period $\tau_B = \hbar/(|F|d)$ corresponding to the time required for the quasi-momentum to scan a full Brillouin zone. The mean velocity in $|n, q(t)\rangle$ is an oscillatory function of time with zero mean. As a consequence, a wave packet prepared with a well-defined quasi-momentum in the n th band will also oscillate in position with an amplitude $\Delta_n/(2|F|)$ where Δ_n is the energy width of the n th band.

In atom experiments, the periodic potential results from the light shift of the ground state of atoms illuminated by a laser standing wave (see figure 4). The laser is detuned far from any atomic resonance so that spontaneous emission can be neglected. The sample of atoms is cooled and prepared in order to have a well-defined initial momentum distribution.

When the atoms are subject only to gravity, the Bloch period τ_B is given by $2\hbar/(mg\lambda_L)$. For this reason Bloch oscillations of an atom in a standing wave are directly related to g : the combination of the periodic optical potential and the linear gravitational potential gives rise to Bloch oscillations at a frequency ν_B given by

$$\nu_B = \frac{mg\lambda_L}{2\hbar} \quad (10)$$

where m is the atomic mass, g is the acceleration of gravity, λ_L is the wavelength of the light producing the lattice and \hbar is the Planck constant. Since λ_L , m and \hbar are well known, the acceleration along the lattice axis can be determined by measuring the Bloch frequency ν_B . Atom Bloch oscillations were directly observed using atoms in an optical lattice in [48, 49] and in [14], where Bloch oscillations have been used for a proof-of-principle measurement of g .

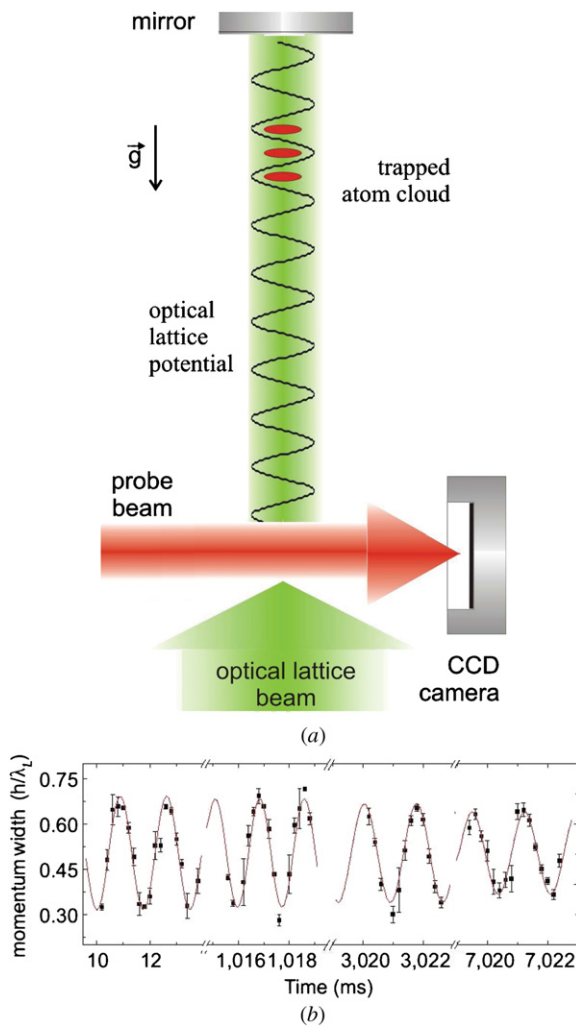


Figure 4. (a) Experimental scheme for producing Bloch oscillations of atoms in a light standing wave. (b) Time evolution of the width of the atomic momentum distribution, showing Bloch oscillation of ^{88}Sr atoms in the vertical one-dimensional optical lattice under the effect of gravity. From the fit of the data a Bloch frequency $\nu_B = 574.568(3)$ Hz is obtained with a damping time $\tau \sim 12$ s for the oscillations. Data have been recorded in Bloch-oscillation experiment of [14].

3. Gravity measurements in metrology, geophysics and geodesy

The gravitational potential $U(\mathbf{r})$ due to a mass distribution $\rho(\mathbf{r})$ in a volume V , that a probe mass m experiences, is defined by

$$U(\mathbf{r}) = -G \int_V \frac{\rho(\mathbf{r}')}{|\mathbf{r} - \mathbf{r}'|} d\mathbf{r}' \quad (11)$$

where G is Newton's gravitational constant. The known acceleration of gravity is defined as the gradient of the potential

$$g_i(\mathbf{r}) = -\frac{\partial U(\mathbf{r})}{\partial x_i} \quad (12)$$

and its vertical component g near the Earth's surface is approximately equal to 9.8 m s^{-2} . The gravity gradient is expressed by a 3×3 tensor

$$T_{ij}(\mathbf{r}) = -\frac{\partial^2 U(\mathbf{r})}{\partial x_i \partial x_j}. \quad (13)$$

This tensor is symmetric and in source-free regions it obeys Laplace's equality:

$$T_{xx} + T_{yy} + T_{zz} = 0. \quad (14)$$

Thus at each point only five of the nine components are independent. Near the Earth's surface T_{zz} is approximately equal to $3 \times 10^{-6} \text{ s}^{-2}$.

Variations in space of these quantities result from peculiarities of the Earth's shape, density distribution and rotation. The determination of the value of g and its variations in space and time is of interest to a wide range of physical sciences related to metrology, geophysics and geodesy. Depending on the length scale of interest, gravity measurements can be performed on the ground or during navigation. While measuring the value of g with a gravimeter satisfies the needs of land-based surveys, during navigation the moving platform accelerations are indistinguishable from the gravitational one. However, the gravity acceleration and the platform acceleration have different spatial characteristics, and the measurement of gravity gradient can discriminate between them. Usually, the objective is to measure the vertical gradient (but not only) of the gravitational field on a moving vehicle and later integrate the signal to obtain the gravity field mapping.

In metrology, the measurement of a force or any physical quantity involving a force is influenced by the gravitational attraction between the masses used in the measurement. Such effects cannot be shielded, gravity being a purely attractive force. This is the reason why the accuracy of the measure of g directly influences the accuracy of the standard units in many metrological fields (mechanics, electricity, thermometry, fluid dynamics), and it is not surprising that increasing efforts are devoted to its precise determination. For metrological purposes, g is regarded as a local physical constant and it is necessary to measure it at every metrological site where standard units influenced by g are determined.

For instance, the standard unit of electric current, the Ampere, is defined using the Watt balance, which in turn requires an accurate measurement of the local gravity [50]. For the standard unit of mass, the metrologists are now proposing a new scheme also based on the Watt balance [51].

The gravitational force is one of the four fundamental forces and the coupling constant G that governs the gravitational attraction between two massive bodies is the least precisely known fundamental physical constant. Many experiments for its determination are based on the measurement of the changes in the acceleration of gravity induced by well-known source masses [52].

Geophysics and geodesy are mainly interested in the distribution of Earth's density. The density profiles of both the solid and fluid parts of the Earth exhibit marked lateral variations. Such heterogeneous, non-equilibrium density distribution causes deviations in both sphericity and gravity field value. The deviation from the spherical shape is partly due to the Earth's rotation, which flattens it at the poles giving it the shape of an ellipsoid.

The equipotential surface of the Earth's gravity field which best approximates the global mean sea level is termed

geoid. Neglecting the influence of tides and currents, the geoid coincides with the surface to which the oceans would conform over the entire Earth if they could flow beneath land masses and adjust to the combined effect of the Earth's mass attraction and the centrifugal force of the Earth's rotation. If the Earth had a uniform density, the geoid would have the shape of an oblate ellipsoid centered on the Earth's center of mass.

Traditionally geodesy is the discipline mostly concerned with the measurement of the terrestrial gravity field over a wide range of spatial scales. Mapping of the Earth's surface in terms of latitude, longitude and height is in fact referred to a *reference ellipsoid*, which is a mathematically-defined surface approximating the geoid. The deviations between the geoid and the ellipsoid are called the *geoid undulations*, and amount up to ± 100 m. Similarly, the geodetic gravity anomaly is classically defined as the difference between gravity on the geoid and normal gravity on the surface of the reference ellipsoid for the appropriate observation latitude [53]. Height determination in the mapping procedure therefore requires accurate and homogeneous gravity field information, in order to establish unified global height systems and to determine physical heights from the heights of the ellipsoid. These subtle gravity variations are measured in mgal ($1 \text{ gal} = 1 \text{ cm s}^{-2}$).

Inertial navigation and precise orbit determination are other geodetic applications requiring very accurate gravity field knowledge [54]. Inertial navigation consists of measuring the inertial forces experienced by an object and uses these forces to determine completely the trajectory and location of the object from a known initial position. Global Positioning System (GPS) is usually used as navigation tool, however there are a number of environments where GPS is unavailable or undesirable. In inertial navigation systems the position estimate obtained from the on-board accelerometers and gyroscopes is typically limited by knowledge of local gravity, particularly near large gravitational anomalies, as these anomalies can perturb the perceived vertical as determined by the gyroscope. In these circumstances, an on-board gravity gradiometer could correct the inertial navigation system's position estimate.

For the determination of the gravity field at large spatial resolution (>10 km), measurements are required to span large scale ranges, a property which is better attained by performing gravity measurements in navigation. Recently, new perspectives to planet-scale gravity measurements are offered by space-borne, satellite surveys. By the time of completing this review (early 2008), the 5-year-long GRACE mission is close to completion, while the GOCE mission is going to be launched soon. While the GOCE mission will use a dedicated space-borne gravity gradiometer, the GRACE mission deduces gravity gradients using satellite-to-satellite tracking. When combined with height determinations, satellite measurements of the gravity field by GOCE can allow the estimate of very precise, regular and quasi-global sea-surface heights, thus offering important perspectives in climate studies. Such dynamic ocean topography (i.e. the sea level above the geoid) is employed as a proxy for sea current determination and can be assimilated into ocean and climate numerical models [55]. Unlike *in situ* measurements,

these data are global and are collected repeatedly for many years, thus providing unique clues for the understanding of geophysical transport processes and to track the effects of climate change at a planetary scale, such as the significant mass variations of the Antarctic ice sheet and associated global sea-level rise [56]. The data collected in orbit by satellite missions are processed to give a map of the terrestrial gravity potential, which is then extrapolated onto the Earth's surface. Such a processing scheme needs however to be constrained by data collected on the terrestrial surface and/or by airborne gravity surveys.

In solid-earth geophysics, gravity measurements are used to deduce variations in the subsurface mass-density distributions, which can be associated with geological structures or processes. To these ends, the geophysicists' aim is to remove regional gravity effects that mask the local anomalies of interest. Since relative differences in gravity are often all that is important, the reference level can be chosen at an arbitrary height, such as the mean elevation of the area of interest. Differently from geodesy, the geophysical perspective to gravity anomaly is better thought of as the difference between a measured value and a predicted value for the same point derived from some theoretical reference model [57].

Satellite data recalled above are providing geophysicists with unprecedented images of the planet-scale gravity field in terms of data homogeneity, quality and improved resolution. While offering new clues for investigating global geodynamics such as plate interactions and mantle convection, these data also allow the determination of the rheological properties of the Earth's interior (e.g., viscosity, rigidity and density) through exact measurements of lithospheric uplift associated with post-glacial rebound processes [58]. Recent studies have also shown the ability of these images to outline the effects of co-seismic and post-seismic deformation due to ruptures from large earthquakes [59, 60].

At local and regional scales, gravimetry is used for investigating the dynamics of active tectonic areas, the measurements of strain accumulation of inverse or normal faulting during the inter-seismic phase and the observation of pore fluid migration/diffusion due to stress changes. Gravity surveying has also greatly contributed to the understanding of the subsurface structure like granite intrusions and reconnaissance/mapping of sedimentary basins. These latter determinations are crucial for evaluating the potential of shallow, soft terrains to amplify ground shaking during earthquakes.

In ore and oil prospecting, gravity survey used to be the most important geophysical technique, although now it has been partially superseded by seismometry. Exploiting the dependence of seismic velocities on propagation medium's density, the joint inversion of gravity and either passive or active seismic data is now becoming a common practice.

A variety of man-induced physical and chemical processes are known to produce substantial vertical displacements of the Earth's surface and are related to mass or fluid extraction or to subsurface pore fluid flows. Gravity measurements are used in aquifer and reservoir monitoring, observation of subsidence

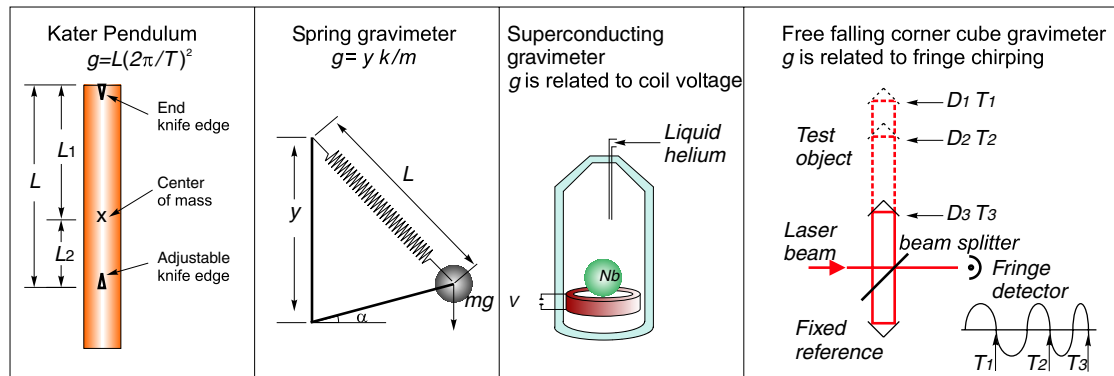


Figure 5. Working principles of the Kater pendulum, spring gravimeter, superconducting gravimeter and free falling corner cube gravimeter.

and mining effects, and monitoring of fluid infiltration and water table rise near sensitive plants.

Very recently observations with a precision of μgal have found an important field of application in volcano monitoring. Reflecting the complex dynamics of subsurface magmatic and hydrothermal fluids, marked variations in the local gravity field have been observed prior and during eruptive episodes of variable size at a number of volcanos worldwide [61, 62].

4. Development of instruments for gravity measurements

To measure gravitational acceleration there are two types of gravimeters one can use to measure the gravitational acceleration: absolute meters, where g can be directly determined by measuring a length and/or a time, and relative meters where g depends on parameters such as spring constants, which cannot be so readily determined (see figure 5). Relative instruments can only detect variations in g in time or space. Early instruments, designed by H Kater [63], were devices utilizing the principle of a reversible pendulum in which the period T , the length L of the ‘mathematical’ equivalent pendulum and g are related by a simple relationship $T = 2\pi\sqrt{L/g}$. The accuracy actually achieved in these measurements is $\Delta g/g \simeq 10^{-4}$. These instruments were used for the first gravimetric survey mapping in the 1930s in Europe and North America [64]. Nowadays, for gravimetric survey, relative spring gravimeters are used, while superconducting and freely falling corner cube gravimeters are used at fixed sites. For the gravity reference networks, particularly important has been the recent use of the Global Positioning System (GPS) for tracking positions and the monitoring of environment effects such as local tides (that can be modeled), groundwater and atmosphere monitoring, subsidence and mass changes in the vicinity.

The sensitivity of a gravimeter is typically quoted in units of $\text{m s}^{-2} \text{ Hz}^{-1/2}$ or $g \text{ Hz}^{-1/2}$, where g is taken as a constant. These units are meant to be the sensitivities for a white-noise-limited process where the precision scales inversely as the square root of the measurement time [65]. For example this means that a $1 \text{ m s}^{-2} \text{ Hz}^{-1/2}$ accelerometer has a raw noise

of 1 m s^{-2} in a 1 Hz bandwidth, giving a precision of about 1 m s^{-2} in 1 s and a precision of about 0.1 m s^{-2} in 100 s.

Current applications of gravity instruments and quality level of gravity reference networks require absolute gravimeters with high sensitivity, at least $\Delta g/g = 10^{-8}$ at 1 s measurement time, and stability within 1 part in 10^8 or 10^9 , on a period of 1 year to 1 decade. At the same time ‘continuous’ acquisition becomes important to measure signals that vary over a period of the order of minutes. Transportability is also a stringent requirement, together with low weight, size and power consumption. Measurements in navigation and satellite in orbit ask for high sensitivity gravity gradient measurements.

In the following we will describe the instruments used so far for gravity measurements, i.e. spring and superconducting gravimeters and ‘free falling corner cube’ gravimeter (table 1) and later we will treat the new sensors based on atom interferometry. Recent information on classical sensor gravimeters can be found in [66], a volume devoted to gravimetry.

5. Classical instruments

5.1. Spring gravimeters

A mass on a massless spring with elastic constant k and total length L has an equilibrium position for a spring elongation δL given by $k\delta L = mg$ and an oscillation period $T = 2\pi\sqrt{m/k}$. This instrument allows us to measure changes in g , by measuring changes in δL , working as a relative meter. The sensitivity of a spring gravimeter is inversely proportional to the square of the oscillation period. Nowadays mass spring gravimeters are designed to have very large T and they are based on ‘zero length springs’ [67]. For this kind of spring the elastic force is directly proportional to the length of the spring ($F = kL$), producing a very large, virtually infinite, oscillation period. In the ‘zero length spring’ gravimeter mounted as in figure 5(b), it is possible to measure changes in g by measuring changes in y .

Spring gravimeters are affected by two main sources of uncertainty. The first is the error in the measurement of y that can cause an error in g as large as $50 \times 10^{-8} \text{ m s}^{-2}$. The second is spring hysteresis which causes drifts in measured

Table 1. Summary of error sources level and technical budgets for most used commercial gravimeters.

	Spring [94]	Superconducting [68, 95]	Free falling [69, 72]
Noise ($\Delta g/g$)/ $\sqrt{\text{Hz}}$	5×10^{-9}	1×10^{-12}	5×10^{-8}
Drift ($\Delta g/g$)	1.5×10^{-6} per month	1×10^{-9} per year	—
Accuracy $\Delta g/g$	—	—	4×10^{-9}
Measurement	Relative	Relative	Absolute
Size (m^3)	0.04	~ 1.5	1.5
Weight (kg)	14	321	127
Power (W)	24	400	350
Error sources	Temperature and random seasonal drift. Calibration varies in time and position	No field operation. Magnetic and electrostatic effects	Thermal drift. Magnetic and electrostatic effects

gravity that can be as large as several hundred μgal per month. Therefore, the meter must be frequently recalibrated.

5.2. Superconducting gravimeters

A superconducting gravimeter is a relative instrument whose principle is to levitate a superconducting sphere in a magnetic field. Gravity changes are compensated by an electrostatic force applied to the sphere to keep it leveled. It is essentially an electro-magnetic spring [68] with a voltage readout signal. The instrument is definitely not a portable device. Furthermore, interruptions such as refilling of liquid helium can reset the calibration factor, i.e. the relation between readout voltage and g . However superconducting gravimeters are very sensitive, with sub- μgal precision, better than the best spring gravimeters and are exceptionally stable in time.

5.3. Free falling corner cube gravimeter

Free fall gravimeters (see figure 5) are absolute instruments that came into their mature technology in the 1980s. The idea is to observe an object in free fall and determine its acceleration. The path length is measured by using an interferometric technique: a freely falling corner cube mirror is the end mirror of one of the arms of a Michelson interferometer. When the cube drops, a sensor reads the interference signal as a function of time [69, 70]. The detected signal is related to the number of half wavelengths of interferometer light covered during the fall by the mirror. For a drop of the mirror (of approximately 20 cm), the values of x and t are recorded and fitted to obtain g .

The main sources of error are the uncertainty in the knowledge of the interferometer laser wavelength λ , electronic counting and timing errors, ground acceleration and unavoidable non-gravitational forces. The last two are typically dominating and they are the real causes of the limit in the accuracy of this instrument. The errors due to ground acceleration or microseisms are of the order of $10^{-6}g$ around 0.1–0.2 Hz (3–8 s period signal). Every acceleration affects the fixed mirror of the interferometer and can map into errors in g . To reduce this noise a ‘super spring’ is used, a device that electronically mimics a 1 km spring corresponding to a 60 s period spring [71]. Since 60 s is much larger than the microseism periods, the mirror motion due to the microseism

is strongly reduced. Non-gravitational forces are essentially electromagnetic forces and air resistance, which are controlled by shielding environmental magnetic fields and by using a falling chamber that moves with the cube during its drop. The best accuracy achieved is 4 μgal [72]. A disadvantage of this instrument is that continuous data acquisition cannot be longer than one week and that the most accurate instruments of this kind are not portable.

5.4. Gravity gradiometers

The first Eötvös gravity gradiometer was developed to measure the difference between the gravitational attraction at two positions about a meter apart. It remained extremely slow to use (8 h per measurement) and very sensitive to external influences such as temperature variations.

The requirement to survey large areas in order to discern the regional variations of the gravity field was often impossible to fulfil due to inaccessibility (over water, large lakes or oceans) or labor and time costs. In navigation either at sea or airborne the accelerations of the moving platform are indistinguishable from a gravitational signal. The requirement of independent kinematic acceleration determination led initially to the development of the airborne gravity gradiometer. Test campaigns performed in the 1980s demonstrated that the airborne gradiometer was a viable tool for gravity mapping [73]. The instrument is a full tensor gravity gradiometer sensor based on a system of pairs of spring accelerometers on a rotating disc. However, due to its cost, it is currently used only by a few exploration companies [74]. The same idea lies behind the ESA mission GOCE where three pairs of accelerometers will be mounted on a satellite orbiting at an altitude of 250 km. The accelerometers are configured to measure the gravity gradient tensor components and, after integration of the signal, to map the gravity field of the Earth [75].

6. Atom-based sensors

6.1. Absolute atom gravimeter

In the first experiment of atom interferometry for acceleration measurement [2, 76], an atomic fountain scheme has been used. Through a careful characterization and elimination of

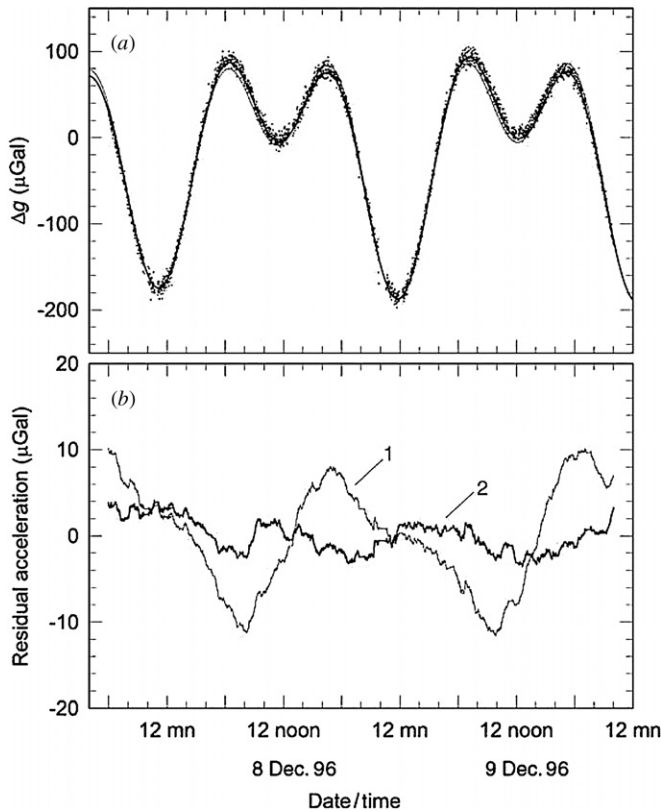


Figure 6. (a) Two days of gravity data measured at Stanford [2]. Each data point represents a 1 min gravity measurement, and the solid lines represent two different tidal models. (b) Residuals of the data with respect to the two tidal models where effects due to changes of the barometric pressure have not been included ($1 \mu\text{gal} \simeq 10^{-9}g$).

systematic effects an absolute uncertainty of $\Delta g < 3 \times 10^{-9}g$ was eventually achieved.

A typical experimental setup is shown in figure 3. In a vacuum chamber at the bottom of the apparatus, a magneto-optical trap [77] collects and cools 10^8 – 10^9 alkali atoms (usually rubidium or cesium) from a vapor produced by getters. After turning the trap magnetic field off, the atomic sample is launched vertically along the symmetry axis of the vacuum tube by using the moving molasses technique [78]. During the launch sequence, atoms are laser cooled to a few μK . Near the apogee of their ballistic flight, atoms interact with the Raman lasers on the three-pulse sequence $\pi/2 - \pi - \pi/2$ which splits, redirects and recombines the atomic wave packets (see section 2.1). At the end of their ballistic flight, the population of the ground state is measured by detecting the light-induced fluorescence emission.

Gravimetry data obtained with the absolute atom interferometer of [2] are shown in figure 6. The data are collected continuously over a period of 3 days, each dot corresponding to data similar to figure 3. The accuracy of the measurement has been tested by the comparison with the value of g obtained in the same laboratory site using a commercial free falling corner cube gravimeter, finding an agreement to within 7 parts in 10^9 . Recently, the same instrument has been improved [3] with a bright source of Cs atoms using Raman

sideband cooling in an optical lattice (an atom cloud at 150 nK of roughly 3 mm^2 area) and with a pulse separation of $T \simeq 0.4 \text{ s}$. The instrument reached an uncertainty of $1.3 \times 10^{-9}g$, representing at the moment the most accurate measurement of absolute acceleration of gravity, and it has been used to test the local Lorentz invariance of post-Newtonian gravity by monitoring Earth gravity.

6.2. Atom gravity gradiometer

The first demonstration of a gravity gradiometer based on atom interferometry is reported in [4, 5]. An atomic gradiometer is a gravimeter where two clouds of laser cooled atoms, separated by a distance D , are used for a simultaneous measurement of local gravity with respect to the common reference frame identified by the wavefronts of the Raman lasers (see figure 7). The instrument detects the differential acceleration Δg and therefore the component of the gravity gradient along the direction of the Raman lasers is simply $\Delta g/D$. For each cloud interference fringes similar to those shown in figure 3 are obtained. The phase difference $\Delta\phi$ between the fringes is proportional to Δg . Increasing the temporal separation between the Raman pulses seismic and acoustic noise completely wash out the fringes. However the two signals, simultaneously detected on the upper and lower accelerometers, remain coupled and preserve a fixed phase relation. As a consequence, $\Delta\phi$ can still be recovered by plotting one series of fringes versus the other. The resulting ellipse is a special case of a Lissajous plot. A nonlinear fit to the ellipse can then be used [79], and the differential phase shift $\Delta\phi$ is obtained from eccentricity and rotation angle of the ellipse fitting the data. In figure 8, elliptic distributions are shown for the apparatus described in [9, 11]. The two atom interferometers at a distance $D = 0.30 \text{ m}$ sense two source masses that can be moved in two different positions with respect to the two atomic clouds: red points are obtained with two source masses close to each other and in between the two atom interferometers, and blue points by moving them far apart. Another atom gravity gradiometer is the one described in [5], where sensitivity has been tested by measuring the Earth's gravity gradient over a period of several days. In [5] for a number of 10^6 atoms per cloud and a separation $D = 1 \text{ m}$ between the clouds, the attained accuracy is 10 E ($1 \text{ E} = 10^{-9} \text{ s}^{-2}$).

6.3. Transportable atom gravimeter prototypes

Prototypes of transportable atom sensors are under development and characterization in several groups around the world. The group of Kasevich at Stanford has developed a transportable instrument for a full determination of the gravity gradient tensor for inertial navigation [80]. At JPL in Pasadena, a compact gravity gradiometer is going to be completed with interesting new solutions for compactness and robustness of the apparatus [81]. An absolute gravimeter has been recently developed in the context of a new Watt balance experiment at LNE-SYRTE, in Paris [82]. The instrument aims at a targeted accuracy $\Delta g/g = 10^{-9}$. Special care was taken in building a compact setup that could be moved

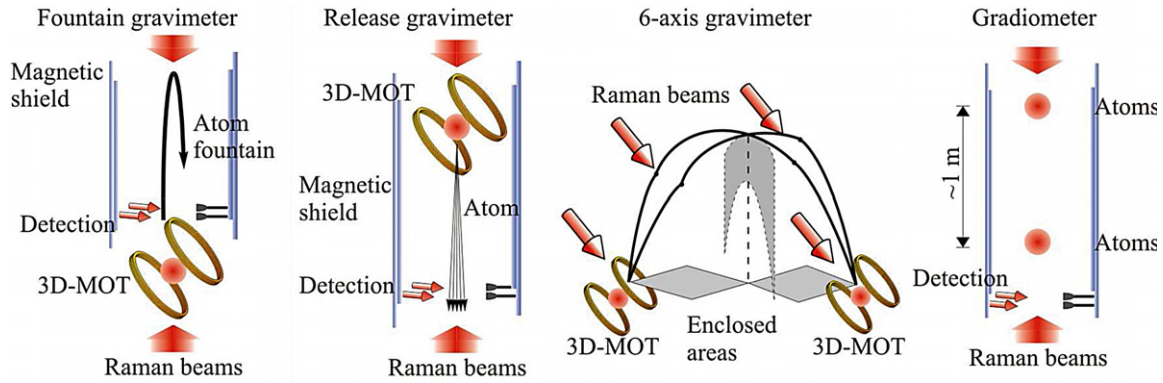


Figure 7. Scheme of gravity sensors based on atom interferometry: absolute measurement of g in a fountain configuration, a release configuration, a 6-axis configuration and a scheme of a gravity gradiometer. Their sensitivities and accuracy are given in table 2.

Table 2. Summary of present sensitivities and accuracy for atom sensor gravimeters and gravity gradiometer of figure 7.

	Fountain [2, 3]	Release [82]	6-Axis sensor [83]	Gradiometer [5, 11]
Sensitivity	$1.1 \times 10^{-8} g/\sqrt{\text{Hz}}$	$1.4 \times 10^{-8} g/\sqrt{\text{Hz}}$	$1.5 \times 10^{-6} g/\sqrt{\text{Hz}}$	$4 \times 10^{-9} (g/m)/\sqrt{\text{Hz}}$
Accuracy	$3 \times 10^{-9} g$	—	—	—

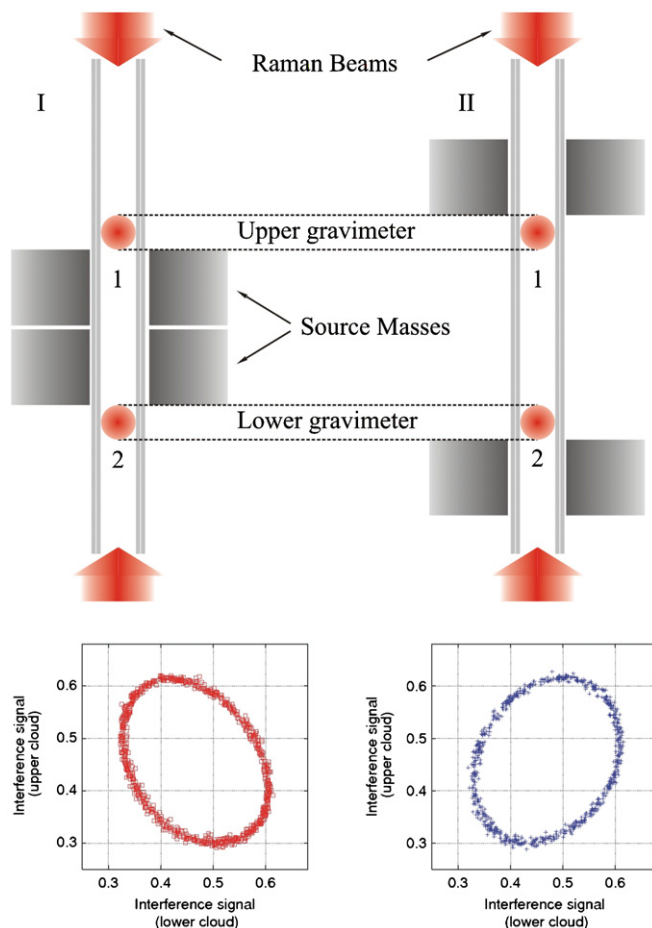


Figure 8. Data distributed along an ellipse obtained by plotting the readout of the upper interferometer against the readout of the lower interferometer. The data are recorded with source masses in two different positions with respect to the sensor: the red points (left) are obtained with two cylindrical source masses close to each other and in between the two atom interferometers, and the blue points (right) by moving them far apart. The data have been reported in [9, 11].

and operated close to the Watt balance. The instrument has an interrogation time $T = 50$ ms and it has now reached a sensitivity of $1.4 \times 10^{-8} g$ at 1 s, enabling a statistical uncertainty of about $1 \times 10^{-9} g$ after 100 s of integration. Presently, the short-term sensitivity is limited by mechanical vibrations.

LNE-SYRTE group is also operating a compact atom interferometer providing a full inertial base, able to measure all six axes of inertia (the three components of acceleration and the three components of rotation) within the same apparatus [83]. Up to now, atom interferometers have only been proven to be sensitive to a single inertial quantity (e.g., acceleration or rotation along one single axis), although intrinsically sensitive to both acceleration and rotation. The principle of such an inertial sensor is illustrated in figure 7. Its present sensitivity is $1.4 \times 10^{-7} \text{ rad s}^{-1}$ to rotation and $6.4 \times 10^{-7} \text{ m s}^{-2}$ to acceleration in 10 min averaging time.

A new portable gravimeter is under construction within the European project FINAQS (Future Inertial Atomic Quantum Sensors); the instrument aims at an accuracy in the range of 1 part in 10^{10} [84], an order of magnitude improvement over the best current instruments.

6.4. Measurement of gravitational constant G

In metrology the determination of the gravitational constant is one of the oldest and most intriguing problems. The CODATA-2006 recommended value for G is $6.674 28(67) \times 10^{-11} \text{ m}^3 \text{ kg}^{-1} \text{ s}^{-2}$ [52]. Despite the large number of experiments realized since 1798, when Cavendish performed the first measurements, G is still affected by an uncertainty of 100 ppm, much higher than that of any other fundamental constant. Considering the most recent experiments, the results differ by several hundreds ppm. Among the possible sources for this unexplained discrepancy, one in particular appears more critical. The majority of the experiments performed so

far are based on macroscopic suspended masses. Systematic effects and parasitic couplings in suspending fibers are not well understood and could be responsible for the observed discrepancies.

The gravitational acceleration induced by moving masses was first observed with atoms at Yale by Kasevich's group [10]. A new experiment in Firenze, proposed in [23], was accurately designed in order to have a better control on the systematic errors and to achieve an uncertainty of 10^{-4} [9, 11]. In the experiment freely falling rubidium atoms are used as probes of the gravitational field induced by source masses. From the differential acceleration measurements, and from the knowledge of the added mass distribution, it is possible to determine the value of G . In that experiment two sets of source masses are symmetrically arranged in a cylindrical geometry around the vacuum tube where atoms are freely falling and can be vertically moved with high precision. They are positioned close to the atomic trajectories and generate a well-known gravitational field [85]. For the determination of G , the source masses signal is detected as variation of the gradient of gravity acceleration. If g_{DW} and g_{UP} are the gravity acceleration values at the height of the lower and upper interferometers the relative phase shift is $\Delta\varphi = k_{\text{eff}}(g_{\text{DW}} - g_{\text{UP}})T^2$. For the determination of G a double differential scheme is implemented. The measurements are repeated twice with atom clouds at the same point but the two source masses at different positions, so that all contributions that are constant in time during the measurement cycle, like rotational or gradient contribution, should cancel out. The change of the local acceleration due to the added gravitational potential can be measured, thus allowing to determine the gravitational constant G , once the source mass-density distribution and their positions are well known. At present the best result in the atom interferometer measurement of G has been given in [11]. The value reported in this work is $G = 6.667 \times 10^{-11} \text{ m}^3 \text{ kg}^{-1} \text{ s}^{-2}$, with an estimated statistical uncertainty of $\pm 0.011 \times 10^{-11} \text{ m}^3 \text{ kg}^{-1} \text{ s}^{-2}$ and a systematic uncertainty of $\pm 0.003 \times 10^{-11} \text{ m}^3 \text{ kg}^{-1} \text{ s}^{-2}$. The result is consistent with the CODATA-2006 recommended value within 1 standard deviation. The main contribution to the systematic error derives from the positioning accuracy of the source masses. This error can be reduced by one order of magnitude once the position of source masses is measured with high resolution methods like laser tracker technique.

6.5. Small spatial scale measurement

The possible deviations from the Newtonian gravitational potential between two point masses are usually described by adding a Yukawa-type term

$$V(r) = -G \frac{m_1 m_2}{r} (1 + \alpha e^{-r/\lambda}), \quad (15)$$

where G is the Newtonian gravitational constant, m_1 and m_2 are the masses and r is the distance between them. The parameter α gives the relative strength of deviations from the Newtonian gravity and λ is its spatial range. Experiments searching for possible deviations have set bounds for the parameters α and λ . Theories predict deviations in the range $\lambda < 1 \text{ mm}$, and recent results using microcantilever detectors lead to extrapolated

limits $\alpha \sim 10^4$ for $\lambda \sim 10 \mu\text{m}$ [86] while for distances below $10 \mu\text{m}$ it was not possible to perform direct experiments so far.

The confinement of ultracold atoms in optical lattices provides clean model systems to study the deviation of the Newtonian law at short distances. The small size and high sensitivity of the atomic probe allow a model-independent measurement at distances of a few μm from the source mass, giving direct access to unexplored regions in the α - λ plane, like in [14, 87], where laser-cooled ^{88}Sr atoms are trapped in a one-dimensional vertical optical lattice. In this experiment, the combination of the periodic optical potential and the linear gravitational potential gives rise to Bloch oscillations (see section 2.2 and figure 4). From the measured Bloch frequency ν_B the gravity acceleration along the optical lattice is estimated with a sensitivity of $1 \times 10^{-6}g$ at 1 s. Although the sensitivity is much lower than that achievable with other atom interferometry sensors, the small spatial extension of the atomic cloud and the possibility to load it into the optical potential at micrometric distance from a surface makes this scheme particularly suitable for the investigation of forces at small spatial scales. Preliminary tests suggest that such a system may allow us to directly test non-Newtonian gravity in the region around $\lambda \sim 5 \mu\text{m}$ with a sensitivity to the α value of 10^3 , more than one order of magnitude lower than the present bounds [88].

7. Future gravity measurements scenario

Accurate gravity measurements find applications in many fields of physics: in metrology for both the definition of SI units and a better knowledge of fundamental constants, in high-precision tests of general relativity, in satellite gravity missions for the geoid mapping and in geophysical studies.

Among the metrological issues in gravimetry, a competitive measurement of G using atom interferometry has been proposed in [89]. The apparatus uses a horizontal configuration for the Raman interrogation beams in order to reduce possible systematic effects associated with source mass positioning. The sensors under development will measure G with a precision approaching 1 part in 10^5 .

Atom interferometry has been recently proposed for laboratory tests of general relativity [12]. Laboratory experiments take place in a well-controlled environment where relativistic effects can be well isolated and measured, noise and systematic error sources studied, and measurements repeated if necessary. Atom interferometry can lead to laboratory tests of general relativity that are competitive with astrophysical tests and potentially superior to them in the long run. Moreover in astrophysical observations there is limited control and often relativistic effects cannot be decoupled.

The setup proposed in [12] is based on a rubidium atom interferometer with an initial targeted accuracy of $10^{-15}g$. These performances will be achieved with an evaporatively cooled atom source, large momentum transfer beam splitters and a 10 m tall vacuum system for the atoms flight, allowing an interrogation time of 1.34 s. Overall sensitivity is both a function of the effective momentum transfer of the atom optic

elements ($\hbar k_{\text{eff}}$), the interrogation time, and the signal-to-noise ratio of the interference fringes. The technical advances in normalized detection methods for atomic clocks and sensors allow us to acquire atom interference fringes with high signal-to-noise ratio limited only by quantum projection noise (atom shot noise) for ensembles of up to 10^7 atoms [90]. Using large momentum transfer beam splitters ($\hbar k_{\text{eff}} = 10\hbar k$) [44, 45], a sample of 10^7 evaporatively cooled atoms and an interrogation time of $T = 1.34$ s, a sensitivity of $7 \times 10^{-13} g$ at 1 s can be reached in a single shot, resulting in $10^{-15} g$ precision after a day of integration time.

Bose–Einstein condensation in dilute atomic gases is also being considered for a new generation of gravitational sensors. The clear difference between the coherence of a BEC and that of a thermal atomic sample is comparable to the difference between a laser and an incoherent light source [37]. In [91], a gravimeter based on a matter-wave resonant cavity loaded with a Bose–Einstein condensate is proposed. The principle is to levitate a free falling atomic sample by providing a controllable acceleration mediated by a coherent atom–light interaction. This acceleration is provided by a sequence of Raman pulses of identical effective wave vector \mathbf{k} interspaced with a duration T that imparts coherently a very well-defined momentum to the collection of atoms. The series of Raman pulses gives an acceleration to the atomic cloud which is monitored by the choice of T . Levitation occurs when the sequence of vertical Raman pulses compensates, on average, the action of gravity. This stabilization is obtained thanks to a fine-tuning of the period between two pulses: after a fixed time, one observes a resonance in the number of atoms kept in the cavity for the adequate period T_0 . The atomic cloud is then well stabilized, and the average Raman acceleration equals the gravitational acceleration. For the resonant period T_0 , the momentum kick imparted during each ‘mirror pulse’ is equal to the momentum acquired in the free fall between two such pulses: $T_0 = 4\hbar k/mg$. Once the period T_0 is known, one can infer the corresponding Raman acceleration hence the gravity acceleration g .

In this scheme the sensitivity scales as $(T_{\text{cav}}/T_0)^{3/2}$, where T_{cav} is the interrogation time of the atoms and T_0 is the duration of a cycle at resonance and, thus, there is an expected improvement of the sensitivity with the atom interrogation time. Nevertheless computation shows that the error in the determination of the gravity acceleration is limited by $\Delta v_r/v_r$, where v_r is the recoil velocity which has been determined with an accuracy as good as a few part in 10^9 for Cs and Rb atoms. On the basis of pure practical considerations, however, BEC sources suffer from the rather tortuous route required to obtain them, although BEC gives the possibility of very long interrogation times.

Let us have a look at the requirements for gravity measurements in geodesy and geophysics. Satellite missions are presently used to map the geoid. In these missions the geopotential second-order derivatives, i.e. the (relative) accelerations of proof masses, are measured along the orbit. The second-order derivatives are then used in an inverse problem to calculate the gravitational potential. The ESA gravity mission GOCE [75] is based on a gravity gradiometer:

proof masses are placed within the satellite and their differential acceleration is monitored. The payload consists in a three-axis gravity gradiometer capable of measuring the diagonal gravity gradient tensor components. The predicted accuracy of the gradiometer is, depending on the axis, 6–100 mE at 1 s between 5 and 100 mHz. A sensor for any GOCE follow-on mission will have to perform even better: sensitivity down to 0.1 mE at 1 s between 0.1 and 100 mHz, and pointing rate knowledge of $4 \times 10^{-11} \text{ rad s}^{-1}$ at 1 s. It is currently believed that these figures cannot be obtained with presently available three-axis gravity gradiometer concepts. Atom interferometry represents a promising technology. Good differential acceleration sensitivities have already been demonstrated on the ground and a significant improvement can be foreseen for operation in space on a satellite in geodetic motion. The sensitivity of these instruments improves with the square of the interrogation time T and, although limited to a few hundreds of milliseconds on the ground because of gravity, in space T can be as large as 10 s. In these conditions, a space gravity gradiometer could in principle achieve a sensitivity better than 1 mE at 1 s at 0.1 Hz. However, a significant miniaturization effort is required to satisfy the compactness needed by a space mission [19].

Users’ interest in terrestrial gravity measurements can be summarized as follows: (1) high resolution prospecting for resource exploration; (2) monitoring of man-induced processes; (3) high resolution geoid mapping (or positioning); (4) investigation of subsurface mass redistribution at local (e.g. volcanos and geothermal systems), regional (post-glacial rebound) and global scales (Earth’s mantle and core).

Data from gravity surveys at the Earth’s surface are usually processed relative to a network of reference stations. The accuracy of measurements from those reference points decreases with time, mostly due to lack of long-term stability of the relative instruments (such as the spring gravimeter) there employed. For such stations, therefore, maintenance of high level of accuracy over long time intervals is a primary requirement.

Recently, continuous micro-gravimetric observations have found a further, important field of application to volcano monitoring. Variations in the local gravity field have been observed prior to and during eruptive episodes, thus suggesting the importance of this geophysical observable as a robust and reliable forecasting tool. Although a unified framework for the interpretation of such changes has yet to be developed, recent studies [92] suggest that these mostly reflect variations in the local density profile associated with the complex dynamics of multi-phase volcanic fluids throughout the volcano’s plumbing system. Physical and mathematical modeling of the dynamics of a compressible, multi-phase magmatic fluid in pre-eruptive conditions also indicates that gravity variations constitute the most significant signal resulting from such processes [93]. From the above observations and theoretical results, it appears that mass redistribution in volcanic systems occurs over time scales spanning the 10^2 – 10^6 s interval (i.e. minutes to months), and have amplitudes ranging from 10 μgal up to hundreds of μgal , which means that a long-term stability instrument is needed.

Subsurface mass redistributions of geodynamical interest occur over time scales spanning the 10^6 – 10^8 s interval (i.e. days to years) and produce gravity variations whose amplitude ranges from a few μgal up to hundreds of μgal . Although subtle, these variations generally precede other surface-detectable signals such as strain variations and/or seismic ground shaking. Taken all together, these considerations thus indicate that the continuous observation of the local gravity field using sensitive instrumentation with μgal accuracy and over long periods (years) is a major goal to be attained toward a better understanding of geodynamic processes and a successful assessment of earthquake and volcanic hazards.

Acknowledgments

Authors acknowledge financial support from Istituto Nazionale di Geofisica e Vulcanologia (INGV, Italy) and EU FINAQS STREP/NEST project contract no 012986.

References

- [1] Kasevich M and Chu S 1992 Measurement of the gravitational acceleration of an atom with a light-pulse atom interferometer *Appl. Phys. B* **54** 321–32
- [2] Peters A, Chung K Y and Chu S 1999 Measurement of gravitational acceleration by dropping atoms *Nature* **400** 849–52
- [3] Müller H, Chiow S W, Herrmann S, Chu S and Chung K-Y 2008 Atom-interferometry tests of the isotropy of post-Newtonian gravity *Phys. Rev. Lett.* **100** 031101
- [4] Snadden M J, McGuirk J M, Bouyer P, Haritos K G and Kasevich M A 1998 Measurement of the Earth's gravity gradient with an atom interferometer-based gravity gradiometer *Phys. Rev. Lett.* **81** 971–4
- [5] McGuirk J M, Foster G T, Fixler J B, Snadden M J and Kasevich M A 2002 Sensitive absolute-gravity gradiometry using atom interferometry *Phys. Rev. A* **65** 033608
- [6] Gustavson T L, Bouyer P and Kasevich M A 1997 Precision rotation measurements with an atom interferometer gyroscope *Phys. Rev. Lett.* **78** 2406–9
- [7] Gustavson T L, Landragin A and Kasevich M A 2000 Rotation sensing with a dual atom-interferometer Sagnac gyroscope *Class. Quantum Grav.* **17** 2385–98
- [8] Fray S, Alvarez Diez C, Hänsch T W and Weitz M 2004 Atomic interferometer with amplitude gratings of light and its applications to atom based tests of the equivalence principles *Phys. Rev. Lett.* **93** 240404
- [9] Bertoldi A, Lempore G, Cacciapuotì L, de Angelis M, Fattori M, Petelski T, Peters A, Prevedelli M, Stuhler J and Tino G M 2006 Atom interferometry gravity-gradiometer for the determination of the Newtonian gravitational constant *Eur. Phys. J. D* **40** 271–9
- [10] Fixler J B, Foster G T, McGuirk J M and Kasevich M A 2007 Atom interferometer measurement of the Newtonian constant of gravity *Science* **315** 74–7
- [11] Lempore G, Bertoldi A, Cacciapuotì L, Prevedelli M and Tino G M 2008 Determination of the Newtonian gravitational constant using atom interferometry *Phys. Rev. Lett.* **100** 050801
- [12] Dimopoulos S, Graham P W, Hogan J M and Kasevich M A 2007 Testing general relativity with atom interferometry *Phys. Rev. Lett.* **98** 111102
- [13] Tino G M 2003 High precision gravity measurements by atom interferometry 2001: *A Relativistic Spacetime Odyssey—Proc. JH Workshop (Firenze, 2001)* ed I Ciufolini, D Dominici and L Lusanna (Singapore: World Scientific) pp 147–58
- [14] Ferrari G, Poli N, Sorrentino F and Tino G M 2006 Long-lived Bloch oscillations with bosonic Sr atoms and application to gravity measurement at the micrometer scale *Phys. Rev. Lett.* **97** 060402
- [15] Tino G M and Vetrano F 2007 Is it possible to detect gravitational waves with atom interferometers? *Class. Quantum Grav.* **24** 2167–77
- [16] Dimopoulos S, Graham P W, Hogan J M, Kasevich M A and Rajendran S 2008 Gravitational wave detection with atom interferometry *Preprint arXiv:0712.1250*
- [17] Dimopoulos S, Graham P W, Hogan J M, Kasevich M A and Rajendran S 2008 An atomic gravitational wave interferometric sensor (AGIS) *Preprint arXiv:0806.2125*
- [18] Peters A, Chung K Y and Chu S 2001 High-precision gravity measurements using atom interferometry *Metrologia* **38** 25–61
- [19] Bresson A, Bidel Y, Bouyer P, Leone B, Murphy E and Silvestrin P 2006 Quantum mechanics for space applications *Appl. Phys. B* **84** 545–50
- [20] Tino G M *et al* 2007 Atom interferometers and optical atomic clocks: new quantum sensors for fundamental physics experiments in space *Nucl. Phys. B* **166** 159–65
- [21] Turyshev S G *et al* 2007 Space-based research in fundamental physics and quantum technologies *Int. J. Mod. Phys. D* **16** 1879–925
- [22] Cheinet P, Pereira Dos Santos F, Petelski T, Le Gouet J, Kim J, Therkildsen K T, Clairon A and Landragin A 2006 Compact laser system for atom interferometry *Appl. Phys. B* **84** 643–6
- [23] Stuhler J, Fattori M, Petelski T and Tino G M 2003 MAGIA—using atom interferometry to determine the Newtonian gravitational constant *J. Opt. B: Quantum Semiclass. Opt.* **5** S75–81
- [24] Clauser J F 1988 Ultra-high sensitivity accelerometers and gyroscopes using neutral atom matter-wave interferometry *Physica B* **151** 262–72
- [25] Bordé C J 1989 Atomic interferometry with internal state labelling *Phys. Lett. A* **140** 10–2
- [26] Berman P R (ed) 1997 *Atom Interferometry* (Chestnut Hill: Academic)
- [27] Miffre A, Jacquy M, Büchner M, Tréneç G and Vigué J 2006 Atom interferometry *Phys. Scr.* **74** C15–23
- [28] Cronin A D, Schmiedmayer J and Pritchard D E 2007 Atom interferometers *Preprint arXiv:0712.3703*
- [29] Bordé Ch J 2002 Atomic clocks and inertial sensors *Metrologia* **39** 435–63
- [30] Fermi E and Marshall L 1947 Interference phenomena of slow neutrons *Phys. Rev.* **71** 666–77
- [31] Carnal O and Mlynek J 1991 Young's double-slit experiment with atoms: a simple atom interferometer *Phys. Rev. Lett.* **66** 2689–92
- [32] Keith D W, Ekstrom C R, Turchette Q A and Pritchard D E 1991 An interferometer for atoms *Phys. Rev. Lett.* **66** 2693–6
- [33] Riehle F, Kisters Th, Witte A, Helmcke J and Bordé Ch J 1991 Optical Ramsey spectroscopy in a rotating frame: Sagnac effect in a matter-wave interferometer *Phys. Rev. Lett.* **67** 177–80
- [34] Kasevich M and Chu S 1991 Atomic interferometry using stimulated Raman transitions *Phys. Rev. Lett.* **67** 181–4
- [35] Rasel E M, Oberthaler M K, Batelaan H, Schmiedmayer J and Zeilinger A 1995 Atom wave interferometry with diffraction gratings of light *Phys. Rev. Lett.* **75** 2633–7
- [36] Chu S, Cohen-Tannoudji C N and Phillips W 1998 Nobel lecture 1997 *Rev. Mod. Phys.* **70** 685–741

- [37] Cornell E A, Wieman C E and Ketterle W 2002 Nobel lecture 2001 *Rev. Mod. Phys.* **74** 875–93, 1131–51
- [38] Kasevich M A 2002 Coherence with atoms *Science* **298** 1363–8
- [39] Weiss D S, Young B C and Chu S 1994 Precision measurement of \hbar/m_{Cs} based on photon recoil using laser-cooled atoms and atomic interferometry *Appl. Phys. B* **59** 217–56
- [40] Moler K, Weiss D S, Kasevich M and Chu S 1992 Theoretical analysis of velocity-selective Raman transitions *Phys. Rev. A* **45** 342–8
- [41] Feynman R P and Hibbs A R (ed) 1965 *Quantum Mechanics and Path Integrals* (New York: McGraw-Hill)
- [42] Antoine C 2006 Matter wave beam splitters in gravito-inertial and trapping potentials: generalized ttt scheme for atom interferometry *Appl. Phys. B* **84** 585–97
- [43] Antoine Ch and Bordé Ch J 2003 Quantum theory of atomic clocks and gravito-inertial sensors: an update *J. Opt. B* **5** S199–207
- [44] McGuirk J M, Snadden M J and Kasevich M A 2000 Large area light-pulse atom interferometry *Phys. Rev. Lett.* **85** 4498–501
- [45] Müller H, Chiow S w, Long Q, Herrmann S and Chu S 2008 Atom interferometry with up to 24-photon-momentum-transfer beam splitters *Phys. Rev. Lett.* **100** 180405
- [46] Cacciapuoti L, de Angelis M, Fattori M, Lempore G, Petelski T, Prevedelli M, Stuhler J and Tino G M 2005 Analog-digital phase and frequency detector for phase locking of diode lasers *Rev. Sci. Instrum.* **76** 053111
- [47] Bloch F 1929 Über die Quantenmechanik der Elektronen in Kristallgittern *Z. Phys.* **52** 555–600
- [48] Ben Dahan M, Peik E, Reichel J, Castin Y and Salomon C 1996 Bloch oscillation of atoms in an optical potential *Phys. Rev. Lett.* **76** 4508–11
- [49] Battesti R, Cladé P, Guellati-Khélifa S, Schwob C, Grémaud B, Nez F, Julien L and Biraben F 2004 Bloch oscillations of ultracold atoms: a tool for a metrological determination of \hbar/m_{Rb} *Phys. Rev. Lett.* **92** 253001
- [50] Kibble B P 1991 Present state of the electrical units *IEE Proc.: Sci. Meas. Technol.* **138** 187–97
- [51] Geneves G *et al* 2005 The BNM Watt balance project *IEEE Trans. Instrum. Meas.* **54** 850–3
- [52] Mohr P J, Taylor B N and Newell D B 2008 CODATA Recommended Values of the Fundamental Physical Constants: 2006 <http://physics.nist.gov/cuu/Constants/codata.pdf>
- [53] Heiskanen W A and Moritz H 1967 *Physical Geodesy* (San Francisco, CA: Freeman)
- [54] Lawrence A (ed) 1998 *Modern Inertial Technology: Navigation, Guidance, and Control* (New York: Springer)
- [55] Tapley B D, Chambers D P, Bettadpur S and Ries J C 2003 Large scale ocean circulation from the GRACE GGM01 Geoid *Geophys. Res. Lett.* **30** 2163
- [56] Velicogna I and Wahr J 2006 Measurements of time-variable gravity show mass loss in Antarctica *Science* **311** 1754–6
- [57] Hackney R I and Featherstone W E 2003 Geodetic versus geophysical perspectives of the ‘gravity anomaly’ *Geophys. J. Int.* **154** 35–43
- [58] Velicogna I and Wahr J 2002 Post glacial rebound and Earth’s viscosity structure from GRACE *J. Geophys. Res.* **107** 2376–87
- [59] Chen J L, Wilson C R, Tapley B D and Grand S 2007 GRACE detects coseismic and postseismic deformation from the Sumatra–Andaman earthquake *Geophys. Res. Lett.* **34** L13302
- [60] Ogawa R and Heki K 2007 Slow postseismic recovery of geoid depression formed by the 2004 Sumatra–Andaman earthquake by mantle water diffusion *Geophys. Res. Lett.* **34** L06313
- [61] Williams-Jones G and Rymer H 2002 Detecting volcanic eruption precursors: a new method using gravity and deformation measurements *J. Volcan. Geoth. Res.* **113** 379–89
- [62] Song T A and Simons M 2003 Large trench-parallel gravity variations predict seismogenic behavior in subduction zones *Science* **301** 630–3
- [63] Kater H 1818 An account of experiments for determining the length of the pendulum vibrating seconds in the latitude of London *Phil. Trans. R. Soc. London* **108** 33–102
- [64] Peters R D 1997 Automated Kater pendulum *Eur. J. Phys.* **18** 217–21
- [65] Allan D W 1966 Statistics of atomic frequency standards *Proc. IEEE* **54** 221–30
- [66] Quinn T J (ed) 2002 Sixth International Comparison of Absolute Gravimeters (ICAG-2001) *Metrologia (Special Issue)* **39** 405–509
- [67] Richter B, Wilmes H and Nowak I 1995 The Frankfurt calibration system for relative calibration *Metrologia* **32** 217–23
- [68] Goodkind J M 1999 The superconducting gravimeter *Rev. Sci. Instrum.* **70** 4131–52
- [69] Niebauer T M, Sagasawa G S, Faller J E, Hilt R and Kloppe F 1995 A new generation of absolute gravimeters *Metrologia* **32** 159–80
- [70] Faller J E 2002 Thirty years of progress in absolute gravimetry: a scientific capability implemented by technological advances *Metrologia* **39** 425–8
- [71] Rinker R L and Faller J E 1984 Super spring—a long period vibration isolator *Precision Measurement and Fundamental Constants II (NBS Special Publication vol 617)* ed B N Taylor and W D Phillips pp 411–7
- [72] Vitushkin L *et al* 2002 Results of the Sixth International Comparison of Absolute Gravimeters, ICAG-2001 *Metrologia* **39** 407–24
- [73] Jekeli C 1993 A review of gravity gradiometer survey system data analysis *Geophysics* **58** 508–14
- [74] van Leeuwen E H 2000 BHP develops airborne gravity gradiometer for mineral exploration *Leading Edge* **19** 1296–7
- [75] Drinkwater M R, Haagmans R, Muzi D, Popescu A, Floberghagen R, Kern M and Fehringer M 2007 The GOCE gravity mission: ESA’s first core Earth explorer *Proc. 3rd Int. GOCE User Workshop (Frascati, Italy, 6–8 November 2006)* vol 62 pp 1–8
- [76] Kasevich M A, Riis E, Chu S and DeVoe R G 1989 RF-spectroscopy in an atomic fountain *Phys. Rev. Lett.* **63** 612
- [77] Raab E L, Prentiss M, Cable A, Chu S and Pritchard D E 1987 Trapping of neutral sodium atoms with radiation pressure *Phys. Rev. Lett.* **59** 2631
- [78] Clairon A, Salomon C, Guellati S and Phillips W D 1991 Ramsey resonance in a Zacharias fountain *Europhys. Lett.* **16** 165–70
- [79] Foster G T, Fixler J B, McGuirk J M and Kasevich M A 2002 Novel method of phase extraction between coupled atom interferometers using ellipse-specific fitting *Opt. Lett.* **27** 951–3
- [80] Young B, Bonomi D S, Patterson T, Roller F, Tran T, Vitouchkine A, Gustavson T and Kasevich M A 2007 Atom optic inertial and gravitational sensors *Laser Science, OSA Technical Digest* (USA: Optical Society of America) page LTuH1
- [81] Yu N, Kohel J M, Keollogg J R and Maleki L 2006 Development of an atom-interferometer gravity gradiometer for gravity measurement from space *Appl. Phys. B* **84** 647–52

- [82] Le Gouët J, Mehlstäubler T E, Kim J, Melet S, Clairon A, Landragin A and Pereira Dos Santos F 2008 Limits to the sensitivity of a low noise compact atomic gravimeter *Preprint* arXiv:[0801.1270](#)
- [83] Canuel B *et al* 2006 Six-axis inertial sensor using cold-atom interferometry *Phys. Rev. Lett.* **97** 010402
- [84] Peters A Contribution of Partner HUB <http://www.finaqs.uni-hannover.de>
- [85] Lamporesi G, Bertoldi A, Cecchetti A, Duhlach B, Fattori M, Malengo A, Pettoruso S, Prevedelli M and Tino G M 2007 Source mass and positioning system for an accurate measurement of G *Rev. Sci. Instrum.* **78** 075109
- [86] Weld D M, Xia J, Cabrera B and Kapitulnik A 2007 A new apparatus for detecting micron-scale deviations from Newtonian gravity *Preprint* arXiv:[0801.1000](#)
- [87] Ivanov V V, Alberti A, Schioppo M, Ferrari G, Artoni M, Chiofalo M L and Tino G M 2008 Coherent delocalization of atomic wave packets in driven lattice potential *Phys. Rev. Lett.* **100** 043602
- [88] Smullin S J, Geraci A A, Weld D W, Chiaverini J, Holmes S and Kapitulnik A 2005 Constraints on Yukawa-type deviations from Newtonian gravity at 20 microns *Phys. Rev. D* **72** 122001
- [89] Biedermann G *et al* 2007 Gravitational physics with atom interferometry *Proc. 18th Int. Conf. on Laser Spectroscopy* (Singapore: World Scientific)
- [90] Santarelli G, Laurent Ph, Lemonde P, Clairon A, Mann A G, Chang S, Luiten A N and Salomon C 1999 Quantum projection noise in an atomic fountain: a high stability cesium frequency standard *Phys. Rev. Lett.* **82** 4619–22
- [91] Impens F, Bouyer P and Bordé C J 2006 Matter-wave cavity gravimeter *Appl. Phys. B* **84** 603–15
- [92] Carbone D, Zuccarello L, Saccorotti G and Greco F 2006 Analysis of simultaneous gravity and tremor anomalies observed during the 2002–2003 Etna eruption *Earth Planet. Sci. Lett.* **245** 616–29
- [93] Longo A, Barbato D, Papale P, Saccorotti G and Barsanti M 2008 Numerical simulation of the dynamics of fluids oscillations in a gravitationally unstable, compositionally stratified fissure *Fluid Motions in Volcanic Conduits: A Source of Seismic and Acoustic Signals (Special Publication vol 307)* ed S J Lane and J S Gilbert (London: Geological Society of London) pp 33–44
- [94] Portable Meter <http://www.LaCosteRomberg.com>
- [95] Francis O and van Damm T 2002 Evaluation of the precision of using absolute gravimeters to calibrate superconducting gravimeters *Metrologia* **39** 485–8